ACS Sustainable Chemistry & Engineering

ACS Editors' Choice

Research Article

pubs.acs.org/journal/ascecg

Terms of Use

The Alpha–Bet(a) of Glucose Pyrolysis: Computational and Experimental Investigations of 5-Hydroxymethylfurfural and Levoglucosan Formation Reveal Implications for Cellulose Pyrolysis

Heather B. Mayes,[†] Michael W. Nolte,[‡] Gregg T. Beckham,[§] Brent H. Shanks,*[,‡,∥] and Linda J. Broadbelt*[,†]

[†]Department of Chemical and Biological Engineering, Northwestern University, Evanston, Illinois 60208, United States

[‡]Department of Chemical and Biological Engineering, Iowa State University, Ames, Iowa 50011, United States

[§]National Bioenergy Center, National Renewable Energy Laboratory, Golden, Colorado 80401, United States

[∥]Center for Biorenewable Chemicals (CBiRC), Iowa State University, Ames, Iowa 50011, United States

Supporting Information

ABSTRACT: As biomass pyrolysis is a promising technology for producing renewable fuels, mechanistic descriptions of biomass thermal decomposition are of increasing interest. While previous studies have demonstrated that glucose is a key primary intermediate and have elucidated many important elementary mechanisms in its pyrolysis, key questions remain. For example, there are several proposed mechanisms for evolution of an important product and platform chemical, 5-hydroxymethylfurfural (5-HMF), but evaluation with different methodologies has hindered comparison. We evaluated a host of elementary mechanisms using a consistent quantum mechanics (QM) level of theory and reveal a mechanistic understanding of this important pyrolysis pathway. We also describe a novel route as a target for catalyst design, as it holds the promise of a more selective pathway to 5-HMF from glucose. We further demonstrate the effect of conformational and structural isomerization on dehydration reactivity. Additionally, we combined QM and experimental studies to address the question of whether only the reactions of β-D-glucose, the cellulose monomer, are relevant to biomass pyrolysis, or if α-D-glucose needs to be considered in mechanistic models of glucose and cellulose pyrolysis. QM calculations show notable differences in elementary mechanisms between the anomers, especially in levoglucosan formation, which provide a means for evaluating experimental yields of α-D-glucose and β-D-glucose pyrolysis. The combined data indicate that both anomers are accessible under pyrolysis conditions. The kinetic and mechanistic discoveries in this work will aid catalyst design and mechanistic modeling to advance renewable fuels from nonfood biomass.

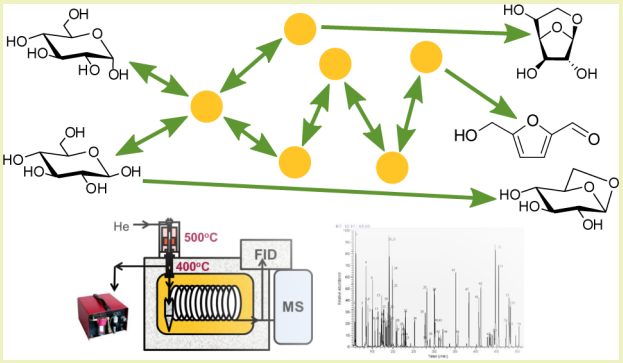

KEYWORDS: *Biomass, 5-HMF, Kinetics, Dehydration, Fuels, Chemicals, Stereoelectronic effects*

INTRODUCTION

Cellulose, a biopolymer of β-D-glucose, is the most abundant component of biomass and is an attractive feedstock to produce carbon-neutral fuels and chemicals.[1] Fast pyrolysis is a promising process for the conversion of biomass to sustainable fuels and chemicals.[2−6] The chemical reactions occurring in fast pyrolysis are important to all thermochemical biomass conversion processes, as pyrolysis is the initial chemical transformation in biomass gasification and combustion.[6] The resulting interest spurred efforts to discern the cellulose pyrolysis product composition and yields[7−10] and reaction mechanisms and kinetics that lead to these products.[8,9,11−13] Elucidating reaction mechanisms will allow improvements to models of biomass pyrolysis,[12,14,15] which can in turn be used for improved process design and optimization for sustainable fuel and chemical production.

The first step toward understanding cellulose pyrolysis reaction mechanisms requires identification of the products formed.[14] Detailed characterization of cellulose pyrolysis products has revealed the main component to be levoglucosan (1,6-anhydro-β-D-glucopyranose), accounting for up to 59 wt % of the product,[7,8,10,16] most of which is believed to form directly from cellulose through a concerted pathway.[12,17] The remaining 41% is composed of water (from dehydration) and products that individually account for less than 7 wt % of the yield, including 6.7 wt % glycolaldehyde, 4.1 wt % of the furanose form of levoglucosan (1,6-anhydro-β-D-glucofuranose), and 2.8 wt % 5-hydroxymethylfurfural (5-HMF), as

Received: February 19, 2014
Revised: April 9, 2014
Published: April 23, 2014

 © 2014 American Chemical Society

reported in the meticulous study by Patwardhan et al. conducted at 500 °C with pure cellulose feed, rapid heating, and minimization of secondary reactions.[7] Identifying the pathways to these important products with lower yields has proved challenging.[13] Vinu and Broadbelt's recent mechanistic model of cellulose pyrolysis offers insight into this question.[12] Their modeling found that the evolution of lower molecular weight products, such as 5-HMF, via a glucose intermediate provided results consistent with experimental yields over a range of relevant pyrolysis temperatures for glucose-based feedstocks of varying chain lengths. This significant finding is consistent with previous work that indicated that glucose is an important intermediate in cellulose pyrolysis[18,19] and that glucose pyrolysis produces many of the low molecular weight species observed in cellulose pyrolysis.[7,20−23] Consequently, understanding glucose pyrolytic decomposition is required to comprehend cellulose and thus biomass thermal conversion.

A number of studies have made great strides toward mapping reaction networks that connect glucose to observed pyrolysis products, many of which were incorporated into Vinu and Broadbelt's model, including a notable series of papers by Paine et al.[21−23] Paine et al. carried out flash pyrolysis of glucose with ^{13}C isotope labeling to determine the origin of specific reactant carbons in the products observed by gas chromatography (GC) and mass spectrometry (MS). From these data, they postulated plausible elementary reaction paths for many observed glucose pyrolysis products, such as glycolaldehyde, acetone, and 5-HMF. Several groups have used quantum mechanics (QM) calculations to obtain transition states (TSs) for glucose thermal decomposition reactions, thus providing evidence that such elementary steps are possible, as well as estimates of energy barriers and reaction kinetic parameters.[24−29] For example, Seshadri and Westmoreland recently published a study evaluating many elementary steps, including mechanisms leading to glycolaldehyde, glyceraldehyde, and levoglucosan (furanose and pyranose forms).[28]

Despite these previous efforts, important questions remain unanswered, likely due to the sheer complexity of the glucose pyrolysis reaction network. Thus, in building their mechanistic model, Vinu and Broadbelt found that data was not available for all glucose decomposition pathways required to capture the observed products, necessitating some hypotheses and parameter fitting for uncertain mechanisms or unavailable kinetics.[12] Some gaps between model predictions and experimental yields of products evolved from glucose intermediates could indicate missing alternate or competing reaction mechanisms, and/or a need for improved kinetics for the reaction mechanisms from glucose included in the microkinetic model. 5-HMF was one of the products for which the model predictions over the range of pyrolysis temperatures studied was not consistent with experimental results and thus merits additional study.

A variety of mechanisms have been proposed for the formation of 5-HMF from glucose under pyrolysis conditions based on theoretical studies.[24,26,27,30] Each QM study used a different level of theory, complicating direct comparisons of different results. A further complication occurs due to calculating reaction barriers using different molecular conformations, which can differ in energy by 10 kcal/mol in some cases, as discussed below. In this work, we use the same method to calculate energy barriers for each of the previously proposed paths from glucose to 5-HMF, as well as two novel paths using the same method. Understanding the mechanism for 5-HMF formation merits study because 5-HMF is one of the main products of glucose pyrolysis[7,20,23,31] as well as a valuable platform chemical.[32−37] A better understanding of its formation could help in process design to maximize its yield not only in pyrolysis but in catalytic routes as well.

Glucose dehydration reactions are central to the formation of 5-HMF as well as a variety of other observed products.[12,20−23,38] We investigated dehydration reactions proposed as part of key glucose pyrolysis reaction mechanisms and similar alternate 1,2-dehydration reactions centered at different positions to provide insight into whether and why certain dehydrations are more likely. We also included the important dehydration reactions that lead to the pyranose and furanose forms of levoglucosan, which are produced from both cellulose and glucose pyrolysis.[7,20] These results underscore the effect of conformational and structural isomerization on reactivity. In deciding which glucose isomers and intermediates should be included in this study, we addressed the fundamental question of whether it is important to consider both α-D-glucose and β-D-glucose as potential reactants in detailed mechanisms of glucose pyrolysis. Cellulose is a monomer of β-D-glucose only,[39] although anomer interconversion is not precluded. In aqueous solution, the anomers come to equilibrium with just over one-third of the population of glucose molecules in the α conformation.[40,41] If the preparation of a glucose sample used as a reactant for pyrolysis includes an aqueous step, the sample is likely to contain both α- and β-D-glucose. Pyrolysis conditions may also allow for interconversion. Seshadri and Westmoreland considered both forms, while other computational studies focus on only β-D-glucose,[9,24,25,30] including studies in the aqueous phase.[42] To determine whether or not both forms should be considered, we followed two lines of investigation, one computational and one experimental. Computationally, we studied several reaction mechanisms leading to observed products, starting from either α- or β-D-glucose, to determine if we could find any significant differences in routes or energy barriers. The mechanisms examined in this effort include paths to 5-HMF, the pyranose form of levoglucosan, and the furanose form of levoglucosan. Experimentally, we compared pyrolysis product distributions from samples that were either primarily α- or β-D-glucose to determine if there are any significant differences in product distributions. This combination of techniques allows us to determine whether both anomers contribute to glucose and cellulose pyrolysis networks and whether there are significant differences in elementary steps that require both anomers to be examined in future mechanistic studies of glucose pyrolysis reactions, which comprise a subset of cellulose reactions.

COMPUTATIONAL METHODS

QM calculations were conducted with Gaussian 09 rev C.[43] The M06-2X[44] functional was used as it has been shown to accurately estimate energy barriers, with a mean signed error of −0.98 kcal/mol for the BBH7 database,[45] and to perform well for biomolecules.[46] We employed the 6-311+G(2df,p) basis set.[47,48] Diffuse functions on hydrogen atoms were not included as they did not appreciably affect results, while diffuse functions and additional polarized functions on the non-hydrogen atoms were included to more accurately model intramolecular hydrogen bonding. The "tight" optimization convergence criteria and "ultrafine" integration grids were specified. Natural population analysis and natural bond orbital (NBO)[49] analysis were performed using NBO 6.0.[50]

All minima were verified to have zero imaginary frequencies, and all TSs have exactly one imaginary frequency. We searched for low-energy

Scheme 1. Elementary Mechanisms for β-D-Glucose Conversion to HMF Considered in This Study[a]

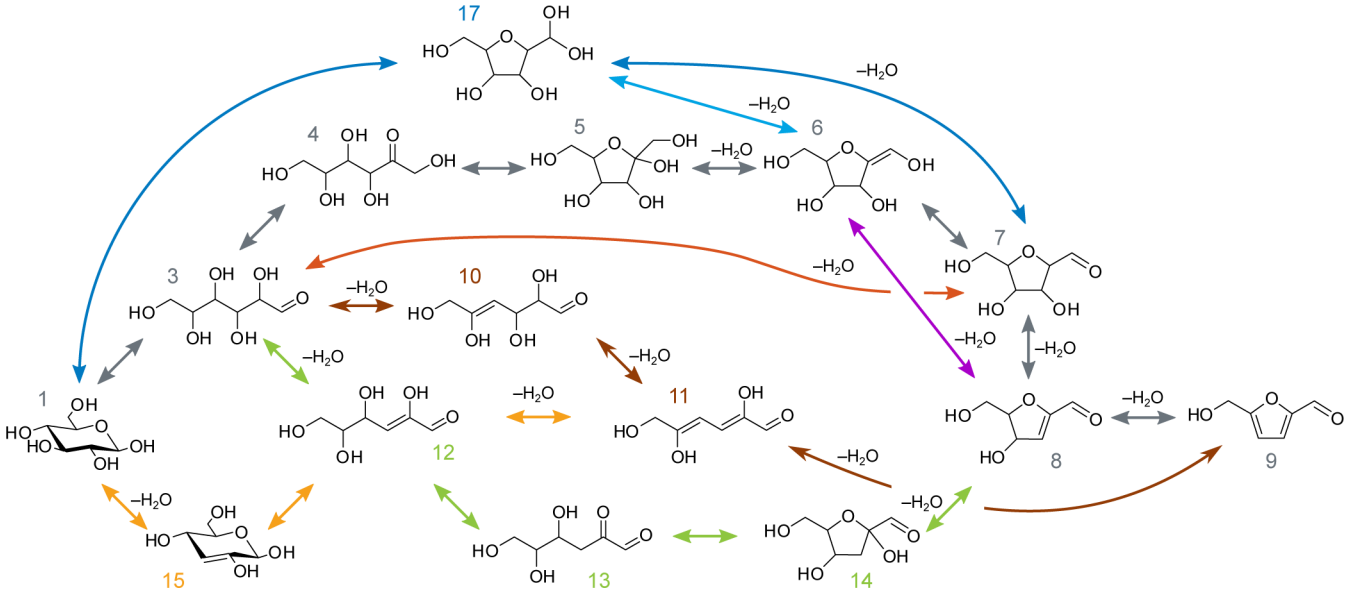

[a]Each arrow represents a single TS.

rotamers of each stationary point and present properties for the lowest-energy conformation found in this work. Additionally, Cartesian atomic coordinates are provided in the Supporting Information for all structures presented. Intrinsic reaction coordinates (IRCs) using the Hessian-based predictor–corrector integration method[51−54] were followed from each TS to connect it with the correct local minima. Normal mode analysis revealed that the low wavenumbers were primarily due to ring puckering and were strongly coupled. Corrections to the harmonic oscillator approximation for internal rotation were not included. Instead, frequencies were scaled with factors reported by Merrick et al.[55] for the M05-2X/6-311+G(2df,p) level of theory, which is most similar to the level of theory employed here. The factors are 0.9663 for zero-point vibrational energy, 0.9444 for fundamental frequencies, 0.9168 for low frequencies (wavenumber less than 260 cm^{-1}), 0.9297 for enthalpy calculations, and 0.9206 for entropy calculations. Reaction rate coefficients were calculated at 100 K intervals between 300 and 1500 K using transition state theory[56] with a 1 M ideal solution as the standard state. The results were fit to the Arrhenius equation to determine the frequency factor (A) and activation energy (E_A). We focus on E_A in our comparison of reactions mechanisms because any inaccuracies in frequency calculations affect A more than E_A, and differences in reaction rate coefficients in a given reaction family are primarily due to differences in E_A. Thus, the relative rate coefficients among families are of greater importance than the absolute values.

The electrostatic environment of glucose pyrolysis, in which the primary reactions are likely to occur in the condensed phase,[12,57] was emulated using the PCM implicit solvent model[58] for ethanol. The electrostatic contribution from ethanol is included because its dielectric constant of 24.852 is similar to the glucose dielectric constant of 21.0 at 423 K.[59,60] Results were also calculated using the lower dielectric constant of 7.43 for implicit tetrahydrofuran (THF), which is similar to the dielectric constant of cellulose,[61] and are presented in the Supporting Information.

EXPERIMENTAL METHODS

α-D-Glucose was purchased from Sigma-Aldrich (96%, 158968 Aldrich). β-D-Glucose was prepared using the method of Reyes et al.[62] adapted from Hudson and Dale.[63] Briefly, 10 g of glucose was added to 1 mL of deionized water and heated to 100 °C. After complete dissolution, 12 mL of hot acetic acid (100 °C) was added to cause precipitation of primarily β-D-glucose. The precipitate was filtered off, washed several times with ethanol, and dried at 40 °C *in vacuo*. The precipitate contained 85% β-D-glucose as measured with a JASCO DIP-370 automatic light polarimeter. The α- and β-D-glucose samples were sieved, and only particles within the size range of 300–500 μm (50–35 mesh) were pyrolyzed.

Glucose samples (200–500 μg) were pyrolyzed at 500 °C in deactivated stainless steel cups using a Frontier Laboratories single-shot micropyrolyzer (model 2020iS). The sample cups were allowed to free-fall by gravity into the preheated furnace. Helium was used as a carrier gas to quickly sweep volatilized products from the heated reaction zone into the gas chromatograph (GC, Bruker 430-GC). Products were identified using a mass spectrometer (MS, Varian Saturn 2200). After confirming peaks using pure standards, pyrolysis vapors were quantified using a flame ionization detector (FID). CO and CO_2 were quantified using a De-Jaye near-infrared gas analyzer. Char was quantified by weighing the sample cups pre- and post-pyrolysis using a Mettler Toledo microbalance (±0.001 mg). The GC separation was achieved using a medium polarity ZB-1701 column (Phenomenex) with a stationary phase consisting of 86% dimethylpolysiloxane and 14% cyanopropylphenyl. The GC method used a 300 °C injection temperature, 103.5 mL/min He flow rate, and a 100:1 split ratio. The column temperature was initially held at 35 °C for 3 min, heated to 300 °C at 5 °C/min, and finally held at 300 °C for 5 min. The MS operated from m/z 30 to 300. The FID was held at 250 °C with a H_2 flow rate of 30 mL/min and an air flow rate of 300 mL/min. Each sample was run in triplicate, and the errors reported correspond to one standard deviation.

RESULTS

Conversion to 5-HMF. 5-HMF has been identified by multiple groups as a main product of glucose pyrolysis,[7,23,31] yet questions remain regarding the mechanism of its formation. One path that is often suggested proceeds via an initial tautomerization to fructose via ring opening and isomerization.[23,27,31,64−66] Experimental evidence for a fructose intermediate in glucose pyrolysis includes Ponder and Richard's detection of fructose in glucose pyrolysis tar.[31] They further confirmed that pyrolysis of fructose results in higher yields of 5-HMF than pyrolysis of glucose, as would be expected if fructose is the intermediate. Paine et al. confirmed this result using isotopic labeling in co-pyrolysis of approximately equimolar glucose and fructose, finding four times as much 5-HMF

dx.doi.org/10.1021/sc500113m | ACS Sustainable Chem. Eng. 2014, 2, 1461−1473

Scheme 2. Elementary Mechanisms for α-D-Glucose Conversion to HMF Considered in This Study[a]

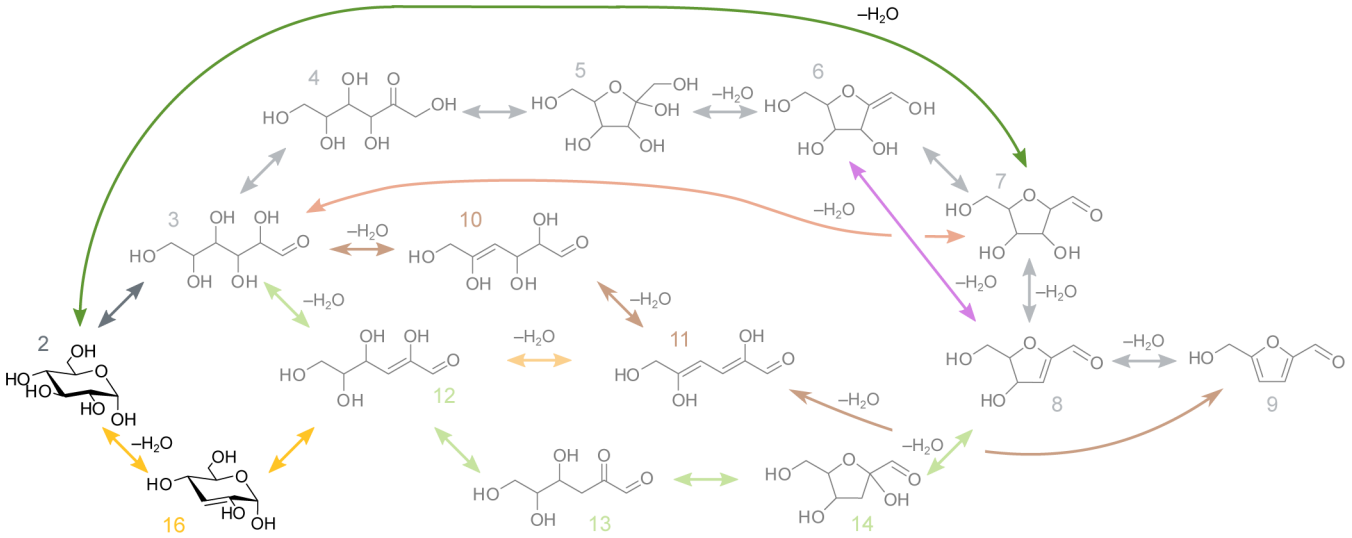

[a]Each arrow represents a single TS. Steps that are common to α- and β-D-glucose are grayed out.

originating from fructose than glucose.[23] These data provide convincing evidence for a more facile "via fructose" route but do not rule out contributions from other mechanisms as well. As Paine et al. noted for furfural formation, computational chemistry studies can provide information about the relative importance of competing elementary mechanisms.[23] A variety of competing elementary mechanisms have indeed been proposed, which are shown in Scheme 1. We investigated each of these mechanisms with the same methodology so they could be compared on an equivalent basis. In the process, we uncovered several novel steps, which are also included in Scheme 1.

The "via fructose" path is represented by the gray arrows in Scheme 1 through the following steps: β-D-glucose (**1**) opens to open D-glucose (**3**), which isomerizes to open D-fructose (**4**), closes to either α- or β-D-fructose (**5**), dehydrates to an enol (**6**), isomerizes to a carbaldehyde (2,5-anhydro-D-mannose) (**7**), loses another water to a dihydrofuran (**8**), and then loses a third water molecule to form 5-HMF (**9**). In addition to the two epimers that can be formed upon ring closure of D-fructose, two epimers of **7** can be formed during isomerization from **6** to **7**, depending on which side of the bond the hydrogen migrates.

There is very little difference in the "via fructose" pathway if the reactant molecule is α-D-glucose (**2**) rather than β-D-glucose (**1**), as shown in Scheme 2. In that scheme, all steps that are common to mechanisms for either anomer are grayed out. For the "via fructose" path, after the initial ring-opening steps, all steps are identical for the two anomers.

In the process of investigating these reactions, we found a TS that directly connects **6** and **8**, shown in purple in Scheme 1, which, as discussed further below, represents an important refinement of the often cited "via fructose" pathway. Recently, Lu et al.[29] investigated epoxide intermediates in an alternate mechanism of 5-HMF formation from fructose but found their formation to have significantly higher energy barriers than mechanisms like the ones shown here, and thus we do not include these mechanisms in this study.

While experimental evidence lends support to a fructose intermediate in 5-HMF formation,[23,31] several alternate mechanisms have been proposed. Shen and Gu[8] proposed that after initial ring opening to **3**, two sequential dehydrations to an enal (**10**) and then dienal (**11**) could be followed by simultaneous ring closure and dehydration to produce 5-HMF (**9**; maroon path in Scheme 1). In contrast to the acyclic dehydration mechanism proposed by Shen and Gu[8] that first removes the C4 hydroxyl group (carbon and oxygen designations follow IUPAC nomenclature,[67] illustrated in previous work[68]), an alternate acyclic dehydration mechanism proposed by Jadhav et al.[26] begins with loss of C3's hydroxyl group to form **12** (light green path in Scheme 1). In that mechanism, dehydration to **12** is followed by enol-keto isomerization to **13**, ring closure to a furan (**14**), and dehydration to **8**. The final step from **8** to 5-HMF (**9**) employs the same step as in the "via fructose" path. Ring closure to **14** could result in two different stereoisomers.

The order of dehydration in Shen and Gu's scheme could be exchanged, starting with loss of the C3 hydroxyl group and then the C4 hydroxyl group, following the path from **3** to **12** to **11**, before simultaneous dehydration and ring closure to 5-HMF (**9**). Zhang et al.[30] recently performed DFT studies of this mechanism, which is also similar to one of the two paths to 5-HMF that Vinu and Broadbelt[12] incorporated into their microkinetic model of cellulose pyrolysis. Their other path to 5-HMF involved initial dehydration of β-D-glucose to the cyclic enol **15** before ring opening to **12** (orange path in Scheme 1), followed by a second dehydration to **11**, and then combined dehydration and ring closure to 5-HMF as in the previously described acylic dehydration path (maroon path in Scheme 1) to join the path similar to **12** to **11** to **9**. For α-D-glucose, dehydration to a cyclic enol yields an epimer of **15** (**16**), shown in yellow in Scheme 2.

Wang et al.[9] also proposed a mechanism that begins with ring opening, which is then followed by a combined dehydration and cyclization step that converts open D-glucose (**3**) directly to the carbaldehyde (**7**; red arrow in Scheme 1). Wang et al.[9] report a TS wherein the C5 hydroxyl group is lost as the carbaldehyde is formed. The carbaldehyde can also be formed by loss of the C2 hydroxyl. We examined both options in this study.

Table 1. Kinetic Parameters[a] for Elementary Steps Shown in Schemes 1 and 2

	forward direction			reverse direction		
reaction	E_A	A	$k_{500\ °C}$	E_A	A	$k_{500\ °C}$
1 ↔ 3	47.0	3.9×10^{13}	2.0×10^{00}	35.7	2.6×10^{11}	2.0×10^{01}
2 ↔ 3	47.6	4.6×10^{13}	1.6×10^{00}	35.6	1.4×10^{11}	1.2×10^{01}
3 ↔ 4	35.1	2.3×10^{11}	2.7×10^{01}	41.1	9.7×10^{11}	2.3×10^{00}
4 ↔ β-5	37.6	1.3×10^{12}	2.9×10^{01}	42.1	3.4×10^{13}	4.1×10^{01}
4 ↔ α-5	39.5	1.1×10^{12}	6.9×10^{00}	44.8	6.2×10^{13}	1.3×10^{01}
β-5 ↔ 6 + H_2O	49.7	1.5×10^{13}	1.4×10^{-01}	33.9	6.2×10^{06}	1.6×10^{-03}
α-5 ↔ 6 + H_2O	56.5	3.5×10^{14}	3.7×10^{-02}	39.8	6.3×10^{07}	3.4×10^{-04}
6 ↔ *trans*-7	62.7	8.5×10^{12}	1.5×10^{-05}	65.0	7.6×10^{11}	3.2×10^{-07}
6 ↔ *cis*-7	65.9	3.2×10^{13}	7.4×10^{-06}	70.6	1.6×10^{13}	1.7×10^{-07}
trans-7 ↔ 8 + H_2O	53.3	1.9×10^{12}	1.6×10^{-03}	49.9	4.9×10^{06}	3.8×10^{-08}
cis-7 ↔ 8 + H_2O	85.3	6.8×10^{11}	5.1×10^{-13}	79.3	3.1×10^{05}	1.1×10^{-17}
6 ↔ 8 + H_2O	38.9	7.7×10^{12}	7.5×10^{01}	37.8	1.8×10^{06}	3.8×10^{-05}
8 ↔ 9 + H_2O	61.2	2.7×10^{14}	1.3×10^{-03}	72.0	2.0×10^{08}	8.4×10^{-13}
3 ↔ 10 + H_2O	71.6	2.6×10^{14}	1.4×10^{-06}	67.8	2.7×10^{08}	1.8×10^{-11}
3 ↔ 12 + H_2O	52.3	2.7×10^{12}	4.2×10^{-03}	49.9	6.7×10^{05}	5.3×10^{-09}
10 ↔ 11 + H_2O	56.1	3.2×10^{13}	4.1×10^{-03}	61.1	2.1×10^{07}	1.1×10^{-10}
12 ↔ 11 + H_2O	69.6	1.7×10^{14}	3.6×10^{-06}	73.1	4.6×10^{08}	9.7×10^{-13}
11 ↔ 9 + H_2O	64.1	6.6×10^{11}	5.0×10^{-07}	67.4	7.7×10^{06}	6.7×10^{-13}
12 ↔ 13	67.0	7.4×10^{12}	8.5×10^{-07}	68.9	2.4×10^{13}	7.7×10^{-07}
13 ↔ β-14	34.7	1.0×10^{12}	1.6×10^{02}	41.8	2.9×10^{13}	4.4×10^{01}
13 ↔ α-14	36.0	6.6×10^{11}	4.2×10^{01}	42.4	1.8×10^{13}	1.8×10^{01}
β-14 ↔ 8 + H_2O	56.8	1.6×10^{13}	1.4×10^{-03}	43.7	7.4×10^{06}	3.2×10^{-06}
α-14 ↔ 8 + H_2O	65.9	4.9×10^{14}	1.1×10^{-04}	53.6	2.2×10^{08}	1.6×10^{-07}
1 ↔ 15 + H_2O	72.8	4.8×10^{12}	1.2×10^{-08}	63.1	3.5×10^{06}	5.0×10^{-12}
15 ↔ 12	46.1	9.4×10^{13}	8.4×10^{00}	42.2	2.1×10^{11}	2.6×10^{-01}
2 ↔ 16 + H_2O	73.2	3.9×10^{12}	7.6×10^{-09}	62.8	7.9×10^{05}	1.3×10^{-12}
16 ↔ 12	45.1	1.7×10^{13}	2.9×10^{00}	41.0	6.4×10^{10}	1.6×10^{-01}
3 ↔ *cis*-7 + H_2O (O2 lost)	73.0	1.4×10^{12}	3.1×10^{-09}	72.5	3.2×10^{07}	1.0×10^{-13}
3 ↔ *cis*-7+ H_2O (O5 lost)	59.3	4.4×10^{12}	7.5×10^{-05}	58.8	1.0×10^{08}	2.4×10^{-09}
1 ↔ 17	76.3	4.8×10^{13}	1.2×10^{-08}	74.9	5.8×10^{13}	3.9×10^{-08}
17 ↔ 6 + H_2O	68.2	2.7×10^{14}	1.4×10^{-05}	53.2	6.6×10^{07}	6.1×10^{-08}
17 ↔ *trans*-7 + H_2O	45.2	2.8×10^{13}	4.7×10^{00}	32.4	6.2×10^{05}	4.3×10^{-04}
2 ↔ *trans*-7 + H_2O	65.3	3.4×10^{14}	1.2×10^{-04}	50.2	4.1×10^{06}	2.6×10^{-08}

[a] E_A in kcal/mol; for unimolecular reactions, the units of A and k are s^{-1}; for bimolecular reactions, the units of A and k are $M^{-1}\ s^{-1}$

Schemes 1 and 2 include novel paths that bypass fructose and the open forms of monosaccharides. This path from β-D-glucose shown in blue in Scheme 1 begins with ring contraction from the pyranose form of glucose to a furanose gemdiol (**17**). From there, dehydration to either **7** (blue) or **6** (light blue) is possible. From α-D-glucose, we obtained a TS combining simultaneous ring contraction and dehydration from the pyranose form to **7** (green). From either **6** or **7**, previously described steps can be followed to produce 5-HMF. These ring contraction paths are intriguing. 5-HMF is a valuable platform chemical,[32−36] spurring active research into increasing its yield from glucose, often under low-temperature aqueous conditions.[37,69−72] A problem plaguing this conversion is lack of selectivity.[34,37,65,70] Bypassing reactive intermediates such as open D-glucose through these ring contraction mechanisms could increase the 5-HMF yield. There is some evidence that ring contraction can occur under low-temperature, aqueous conditions; Qian[42] observed a short-lived gemdiol intermediate in a metadynamics simulation of aqueous glucose at 300 K. Here, we present not only the intermediate but also the TSs to and from the gemdiol and the direct ring contraction from α-D-glucose to **7**.

Table 1 provides kinetic parameters for each of the elementary steps in Schemes 1 and 2. As previously noted, uncertainty in the calculated value of A makes it more informative to compare relative rate coefficients, although the low absolute value of some rate coefficients, such as for *cis*-7 ↔ 8 + H_2O, makes it unlikely for that reaction to be relevant to fast pyrolysis, which has a time scale on the order of seconds.[73] Figure 1 provides a free energy diagram for each of these mechanisms, shown on two graphs to increase clarity. The "via fructose" pathway is shown in gray with the "carbaldehyde bypass" in purple on both graphs to aid comparison of barriers for each of the other mechanisms.

The "via fructose" pathway reveals interesting contrasts for epimers of the same species. The first step, ring opening to open D-glucose (**3**), has similar energies (less than 1 kcal/mol difference in E_A) for either β-D-glucose (**1**) or α-D-glucose (**2**). Seshadri and Westmoreland[28] reported a lower energy barrier for the β-D-glucose ring opening than we report here and provided Cartesian coordinates for its TS, which facilitated comparison of energy barriers. Reoptimizing its TS geometry using the same level of theory employed in this work revealed that its TS is marginally higher in energy. The difference in reported energy barriers is likely due to a combination of different levels of theory and different conformations for the reactant (β-D-glucose; reactant conformation not reported by Seshradi and Westmoreland). As with the anomers of D-

dx.doi.org/10.1021/sc500113m | ACS Sustainable Chem. Eng. 2014, 2, 1461−1473

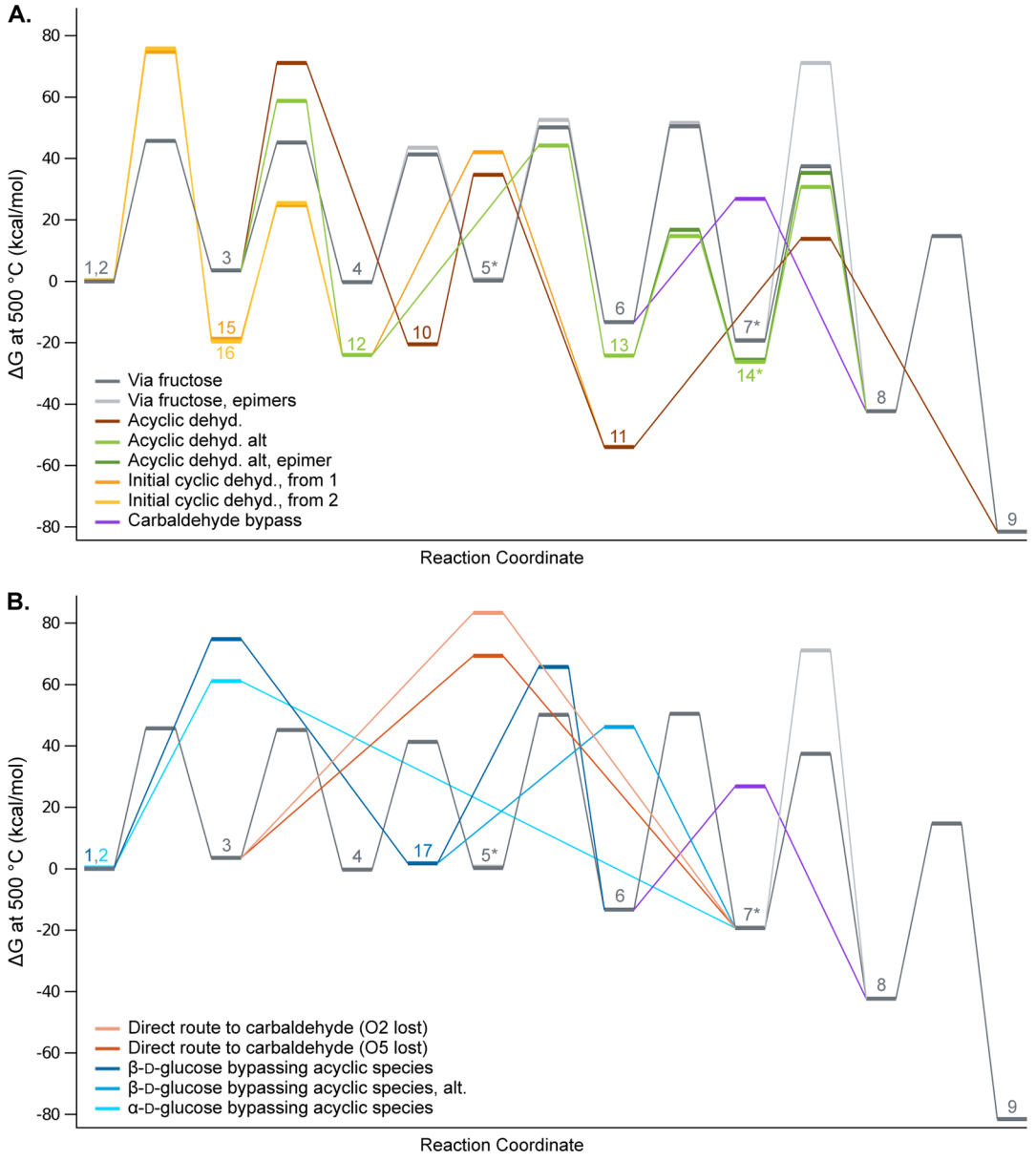

Figure 1. Relative Gibbs free energy at 500 °C for the mechanisms shown in Schemes 1 and 2, calculated with M06-2X/6-311+G(2df,p) and implicit ethanol. The "via fructose" path is shown in gray in both (A) and (B) to facilitate comparison with the other mechanisms, which are shown on two graphs for clarity. The numbers listed on the diagram correspond to the numbered molecules in the schemes. An asterisk indicates a molecule for which two epimers can be formed. The relative energies shown for dehydration products include the water molecule(s) produced.

glucose, the low-energy conformations of the D-fructose anomers are very similar in energy, as expected,[74] with β-D-fructose a few tenths of a kcal/mol lower in free energy (energies for each stationary point are included in the Supporting Information). However, unlike the D-glucose anomers, the anomers of D-fructose display a small difference (~2 kcal/mol) between them for ring opening and closing reactions. The free energies of the epimers of **7** differ by less than 0.2 kcal/mol, with the *trans* carbaldehyde slightly lower in energy. The E_A for **6** to trans-**7** (shown in dark gray in Figure 1) is 3 kcal/mol lower than for the *cis* form (light gray in Figure 1A). A more significant difference between the epimers appears in the next step of the "via fructose" mechanism. For the *trans* conformation, the C2 hydrogen and C3 hydroxyl group that are lost to form **8** are on the same side of the furanose ring, unlike with the *cis* conformation. As a result, the E_A for *trans*-**7** to **8** is 32 kcal/mol lower than from *cis*-**7**. The green "acyclic dehydration" pathway shown in Scheme 1 can create two isomers when **13** forms **14**. As with other stereoisomers, the epimers of **14** have similar free energies, with the β-epimer 0.7 kcal/mol lower in $\Delta G_{500°C}$. The E_A for forming β-**14** from **13** is 1.4 kcal/mol lower than from the α-epimer, and dehydration of β-**14** to **8** is 9 kcal/mol lower. The free energies for β-**14** and its associated TSs are shown in light green in Figure 1A, and the free energies associated with α-**14** are in dark green. The energy barriers we report here have some discrepancies with those reported by Jadhav et al.,[26] which we traced to using lower-energy conformations of reactant molecules in the present study.

The large reaction barrier (E_A of 62.7 kcal/mol) for isomerization from **6** to *trans*-**7** is similar in magnitude to previously published values for this step.[66] Other keto-enol

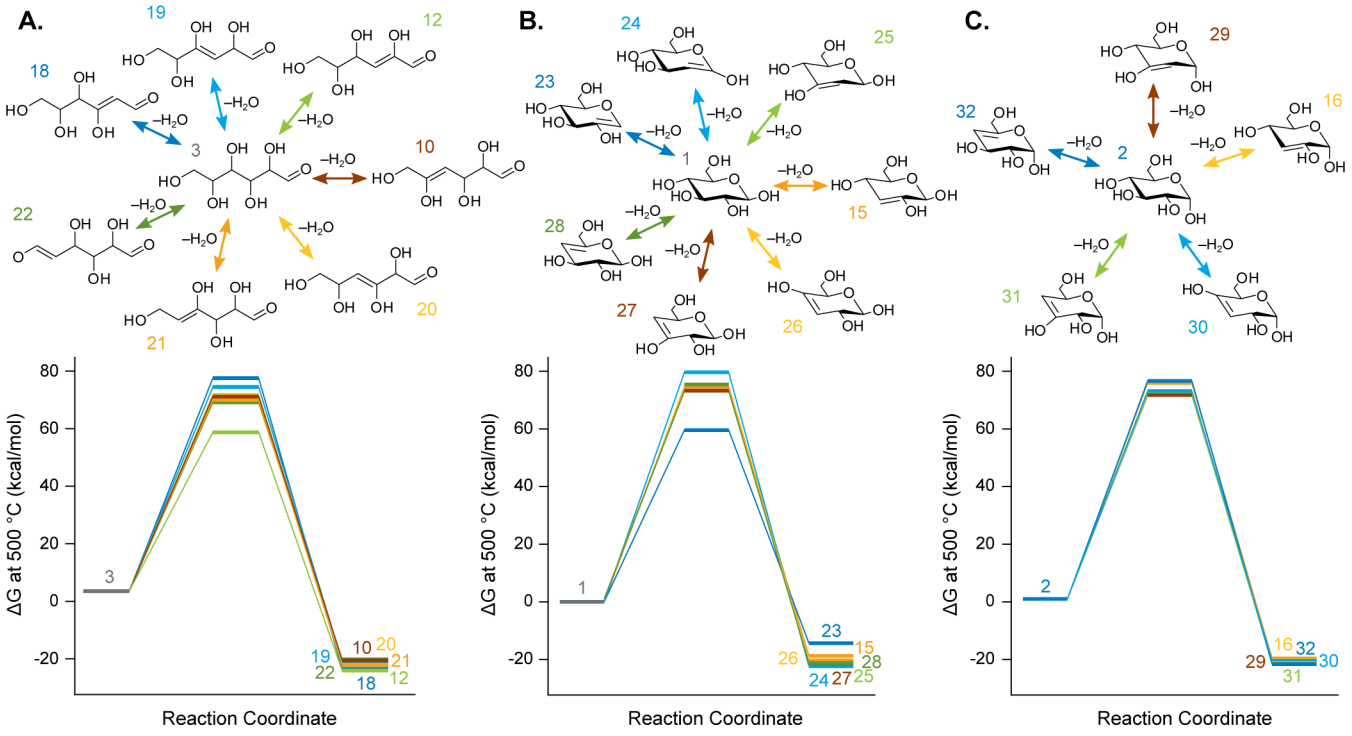

Figure 2. Schemes and free energy diagrams for 1,2-dehydration reactions of (A) the open form of D-glucose (**3**), (B) β-D-glucose (**1**), and (C) α-D-glucose (**2**). Free energies were calculated with M06-2X/6-311+G(2df,p) with implicit solvent, all shown relative to β-D-glucose. Product free energies include organic and water molecules.

tautomerization reactions important in glucose pyrolysis have even larger barriers reported, such as the isomerization of prop-1-ene 1,2,3-triol to glyceraldehyde reported by Seshadri and Westmoreland.[28] Interestingly, for that three-carbon molecule, we found a low-energy "boomerang" TS, described in the Supporting Information, although we did not find such a TS for the **6** to **7** enol-keto isomerization or for the **12** to **13** enol-keto isomerization.

The E_A for the "carbaldehyde bypass" (dehydration of **6** to **8** in one step) of 38.9 kcal/mol is 23.8 kcal/mol lower than the E_A of 62.7 kcal/mol to proceed through **7**, which is typically included in the elementary mechanism for the "via fructose" route under neutral conditions.[31,66] This step not only bypasses one intermediate (which has not been observed to the best of our knowledge) but also bypasses the highest enthalpic barrier in the traditionally presented "via fructose" path.[27,66] Thus, this finding presents an important update to our understanding of this important pyrolysis pathway.

Table 1 reveals that the dehydration of D-glucose (**3**) to **10** or **12** (E_A values of 71.6 and 53.3, respectively) compete with the much lower energy barriers for D-glucose ring closure (E_A of 36 kcal/mol) and isomerization to D-fructose (E_A of 35 kcal/mol). Huang et al.[24] previously reported a barrier for **3** to **10** approximately 10 kcal/mol lower than the value presented here, also based on a DFT study. The discrepancy is primarily due to different conformations used for calculating the energy of **3**; the conformation used by Huang et al. (molecule IM1 in that work[24]) is 9.6 kcal/mol higher in free energy at 500 °C than the lowest energy conformation we found for **3**, underscoring the effect of conformation on calculations of energy barriers. The comparison of energy barriers to form **10** versus **12** highlights differences in electronic environments of structural isomers affecting their reactivities. Unlike in **10**, the double bonds in **12** can be stabilized by significant π bond delocalization. Thus, it is not surprising that we found E_A for dehydration of **3** to **12** to be almost 20 kcal/mol lower than for **3** to **10**. As shown in Schemes 1 and 2, **12** can also be formed by dehydration of either β-D-glucose (**1**) or α-D-glucose (**2**) followed by ring opening (through **15** or **16**, respectively), although Table 1 reports that these paths require overcoming activation energies larger than 70 kcal/mol.

The free energy differences for the direct routes from **3** to **7** are shown in peach (O2 lost) and red (O5 lost) in Figure 1B. Our study confirmed the finding from Wang et al. that the lowest barrier (Table 1) results from loss of the C5 hydroxyl group. In each case, the stereochemistry of the resulting carbaldehyde is *cis*-**7**, which has the higher energy barrier for dehydration to **8** (the light gray path in Figure 1 traces *cis*-**7** to **8**) and an extremely low rate coefficient.

As shown in Figure 1B, the ring contraction TSs in the route to HMF that bypass acyclic species have higher free energies than TSs in the "via fructose" route. It is not surprising that the previously proposed and experimentally supported "via fructose" path has lower energy barriers. However, if a suitable catalyst could be identified to lower the ring contraction reaction barrier, this path could offer a more selective route to HMF by eliminating the opportunity for competing reactions of the bypassed intermediates. Importantly, the carbaldehyde isomer that can be formed is *trans*-**7**, which has the significantly lower dehydration energy barrier to **8** compared to the *cis*-**7** isomer. Snapshots along the ring contraction reaction coordinate are provided in the Supporting Information for the catalysis researcher interested in investigating this path further.

Comparison of 1,2-Dehydration Reactions. As demonstrated by comparing the E_A values for dehydration of **3** to **12** versus dehydration of **3** to **10**, there are significant differences in energy barriers when different hydroxyl groups are removed.

dx.doi.org/10.1021/sc500113m | ACS Sustainable Chem. Eng. 2014, 2, 1461−1473

Table 2. Kinetic Parameters[a] for Elementary Steps Shown in Figure 2

	forward direction			reverse direction		
reaction	E_A	A	$k_{500°C}$	E_A	A	$k_{500°C}$
3 ↔ 18 + H_2O	74.0	1.8×10^{13}	2.1×10^{-08}	74.7	5.1×10^{07}	3.7×10^{-14}
3 ↔ 19 + H_2O	74.4	1.8×10^{14}	1.6×10^{-07}	71.4	2.7×10^{08}	1.7×10^{-12}
3 ↔ 20 + H_2O	67.5	1.2×10^{13}	9.3×10^{-07}	62.2	3.4×10^{06}	8.4×10^{-12}
3 ↔ 21 + H_2O	69.3	1.3×10^{14}	3.2×10^{-06}	63.8	1.5×10^{07}	1.4×10^{-11}
3 ↔ 22 + H_2O	68.2	1.1×10^{14}	5.3×10^{-06}	65.6	3.0×10^{08}	8.2×10^{-11}
1 ↔ 23 + H_2O	62.0	8.7×10^{13}	2.5×10^{-04}	47.0	3.4×10^{07}	1.7×10^{-06}
1 ↔ 24 + H_2O	80.3	3.4×10^{13}	6.4×10^{-10}	73.1	1.2×10^{07}	2.4×10^{-14}
1 ↔ 25 + H_2O	77.7	2.1×10^{14}	2.2×10^{-08}	70.4	1.5×10^{08}	1.8×10^{-12}
1 ↔ 26 + H_2O	77.7	1.8×10^{14}	1.9×10^{-08}	69.7	1.5×10^{08}	2.8×10^{-12}
1 ↔ 27 + H_2O	76.3	1.3×10^{14}	3.4×10^{-08}	68.9	8.1×10^{07}	2.5×10^{-12}
1 ↔ 28 + H_2O	74.0	3.1×10^{13}	3.7×10^{-08}	65.2	7.7×10^{06}	2.8×10^{-12}
2 ↔ 29 + H_2O	75.1	2.2×10^{14}	1.2×10^{-07}	66.6	5.8×10^{07}	8.3×10^{-12}
2 ↔ 30 + H_2O	77.7	4.6×10^{14}	4.9×10^{-08}	69.6	2.5×10^{08}	5.0×10^{-12}
2 ↔ 31 + H_2O	76.1	3.4×10^{14}	1.0×10^{-07}	68.8	1.9×10^{08}	6.8×10^{-12}
2 ↔ 32 + H_2O	74.6	6.0×10^{12}	4.7×10^{-09}	65.0	5.3×10^{05}	2.2×10^{-13}

[a] E_A in kcal/mol; for unimolecular reactions, the units of A and k are s^{-1}; for bimolecular reactions, the units of A and k are M^{-1} s^{-1}

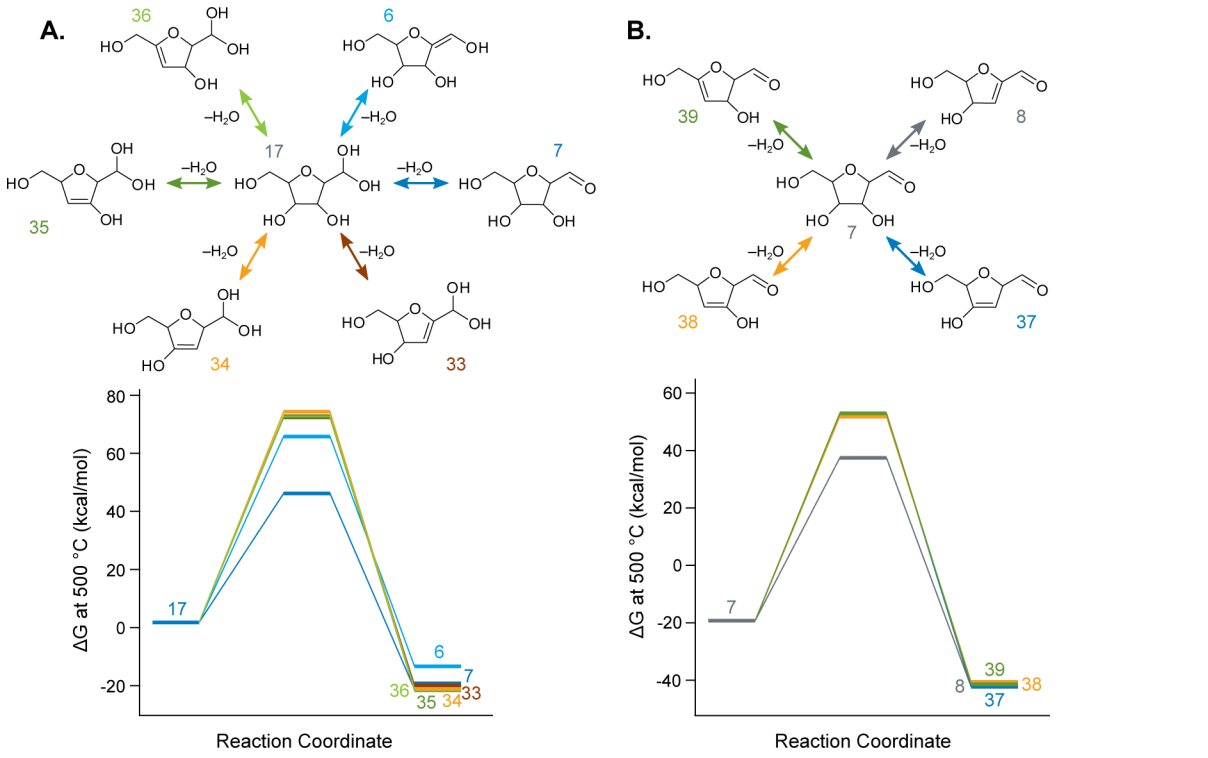

Figure 3. Schemes and free energy diagrams for 1,2-dehydration reactions of two intermediates in glucose to 5-HMF routes: (A) Gemdiol (**17**) and (B) carbaldehyde (**7**). Free energies were calculated with M06-2X/6-311+G(2df,p) with implicit solvent, all shown relative to β-D-glucose. Product free energies include organic and water molecules.

While that difference is not surprising due to the presence or absence of stabilizing π bonds, quantifying these differences merits careful study due to the importance of dehydration reactions in glucose and cellulose pyrolysis.[7,16,23,75]

Figure 2A compares seven possible dehydration reactions of the open form of D-glucose based on their relative free energies, with kinetic parameters in Table 2 for the reactions not already included in Table 1. The lowest barrier found for this set of dehydration reactions is formation of **12**, with an E_A of 52.3 kcal/mol (shown in Table 1). Interestingly, both **12** and **18** have a C2-C3 double bond, yet the E_A to form **18** is significantly higher at 74.0 kcal/mol. In the TS for **3** to **12**, the C2 hydrogen is lost, and the C2-H bond is highly delocalized, as shown by the NBO analysis. Unlike with the other TSs, the hydrogen abstracted from a carbon atom is aligned to benefit from delocalization of an anomeric oxygen lone pair, making this TS uniquely stable.

There are also a variety of 1,2-dehydration reactions possible for α- and β-D-glucose. The various dehydration barriers from β-D-glucose to cyclic enols (Figure 2B and Table 2) are clustered together, with E_A to **24** 4.0 kcal/mol higher than the median and E_A to **23** 14.3 kcal/mol lower than the median. Interesting, both of these dehydration barriers result in a cyclic enol with the double bond between C1 and C2. The key

dx.doi.org/10.1021/sc500113m | ACS Sustainable Chem. Eng. 2014, 2, 1461−1473

Table 3. Kinetic Parameters[a] for Elementary Steps Shown in Figure 3

	forward direction			reverse direction		
reaction	E_A	A	$k_{500°C}$	E_A	A	$k_{500°C}$
16 ↔ 33 + H_2O	74.3	1.7×10^{14}	1.6×10^{-07}	62.8	5.7×10^{06}	9.6×10^{-12}
16 ↔ 34 + H_2O	74.4	5.8×10^{13}	5.2×10^{-08}	66.8	1.1×10^{07}	1.4×10^{-12}
16 ↔ 35 + H_2O	74.3	2.0×10^{14}	1.9×10^{-07}	66.9	3.3×10^{07}	3.9×10^{-12}
16 ↔ 36 + H_2O	69.5	6.1×10^{12}	1.4×10^{-07}	60.1	3.4×10^{05}	3.4×10^{-12}
7 ↔ 37 + H_2O	72.4	2.5×10^{13}	8.2×10^{-08}	69.0	7.3×10^{07}	2.2×10^{-12}
7 ↔ 38 + H_2O	69.4	5.9×10^{12}	1.4×10^{-07}	64.4	1.8×10^{07}	1.1×10^{-11}
7 ↔ 39 + H_2O	69.9	3.9×10^{12}	6.6×10^{-08}	64.3	4.6×10^{06}	2.9×10^{-12}

[a] E_A in kcal/mol; for unimolecular reactions, the units of A and k are s^{-1}; for bimolecular reactions, the units of A and k are M^{-1} s^{-1}

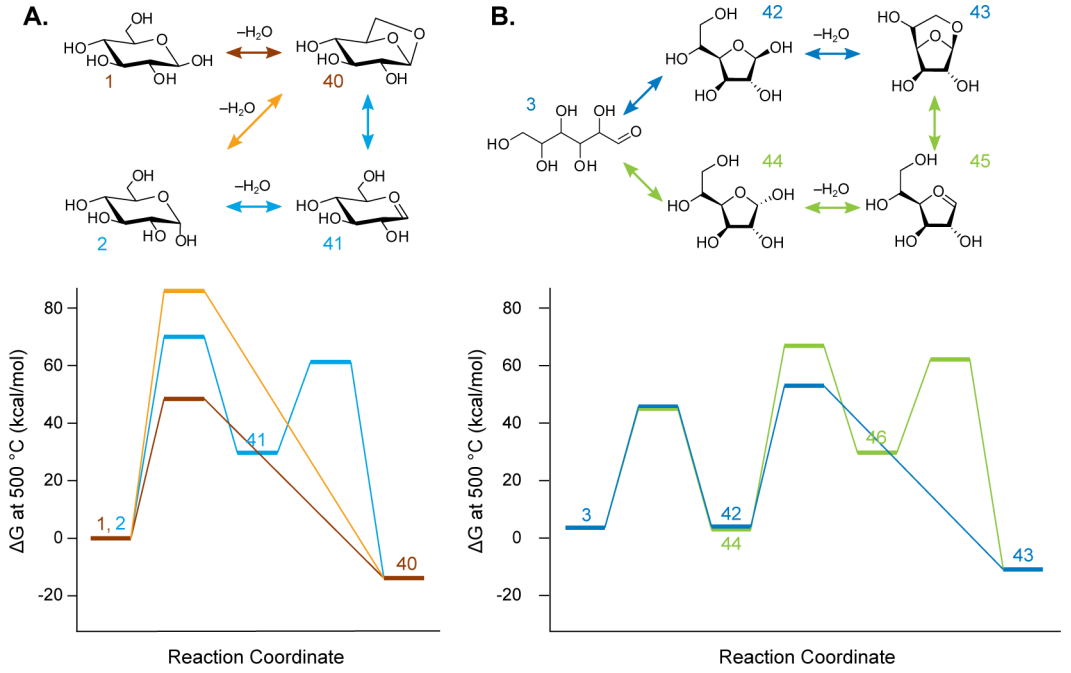

Figure 4. Schemes and free energy diagrams for formation of (A) pyranose and (B) furanose forms of levoglucosan from glucose. Free energies were calculated with M06-2X/6-311+G(2df,p) with implicit solvent, all shown relative to β-D-glucose. Product free energies include organic and water molecules.

feature of these two dehydration reactions is that in each case, a substituent of the anomeric carbon is lost. The anomeric carbon has a higher positive charge than all the other carbons due to electron donation to its two adjacent oxygen atoms.[68,76] The formation of **24** is relatively more difficult, requiring removal of an electron-donating hydrogen from the anomeric carbon. In contrast, as the electronegative hydroxyl group is removed during the formation of **23**, the increased partial charge on C1 is stabilized by the ring oxygen (O5). The TS for dehydration of **1** to **23** is further stabilized by hydrogen bonding from the hydroxylmethyl group. Zhang et al.[30] recently evaluated four of these seven reactions (excluding dehydration of **1** to **23**), obtaining similar barriers to those presented here. This work also corroborates previously reported barriers for three possible dehydration reactions of cellotriose (not involving anomeric substituents) to produce cyclic enols.[77]

The orientation of the anomeric hydroxyl group for α-D-glucose disallows 1,2-dehydration involving the removal of the C1 hydroxyl with the C2 hydrogen or removal of the C2 hydroxyl with the C1 hydrogen because the C1 and C2 hydroxyl groups are in a *cis* orientation. Thus, there are five, not seven, 1,2-dehydration reactions of α-D-glucose resulting in a cyclic enol, all involving chemically similar carbons losing substituent groups. Thus, it is not surprising that the barriers for the five dehydration reactions shown in Figure 2C are similar (Table 2). Assary and Curtis[27] have shown that these reaction barriers can be lowered if a water molecule is present to facilitate the reaction. Under pyrolysis conditions (approximately 500 °C), little water is expected to be present, as it would readily evaporate, so explicit water molecules are not included except as reaction products.

Additional 1,2-dehydration reactions from the carbaldehyde (**7**) and gemdiol (**17**) are shown in Figure 3 with kinetic parameters in Table 3. As is clear from the free energy diagram, none of these alternate 1,2-dehydration steps have a lower barrier than those shown in Table 1.

Conversion to Levoglucosan. Levoglucosan is an abundant product of cellulose and glucose pyrolysis.[3,7,18,23,57] Both the pyranose form (**40**, Figure 4) and furanose form (**43**) of levoglucosan are observed, with greater yields of the pyranose form, as shown below and in previous studies,[7,18,57,73] which can be formed in one step via dehydration of β-D-glucose (**1**).[9,23,24,28] Additional forms of levoglucosan are possible, such as 2,6-anhydro-β-D-glucopyranose and 3,6-anhydro-β-D-glucopyranose. However, to the best of our knowledge, they have not been observed or

dx.doi.org/10.1021/sc500113m | ACS Sustainable Chem. Eng. 2014, 2, 1461−1473

Table 4. Kinetic Parameters[a] for Elementary Steps Shown in Figure 4

	forward direction			reverse direction		
reaction	E_A	A	$k_{500°C}$	E_A	A	$k_{500°C}$
1 ↔ 40 + H_2O	48.2	1.4×10^{13}	3.2×10^{-01}	37.5	1.4×10^{08}	3.3×10^{-03}
2 ↔ 40 + H_2O	84.3	7.5×10^{12}	1.1×10^{-11}	72.7	3.2×10^{07}	8.6×10^{-14}
2 ↔ 41 + H_2O	76.5	1.7×10^{15}	3.7×10^{-07}	14.1	5.6×10^{07}	5.7×10^{03}
41 ↔ 40	24.9	2.2×10^{11}	2.0×10^{04}	75.8	2.8×10^{13}	1.0×10^{-08}
3 ↔ 42	34.3	9.7×10^{10}	1.9×10^{01}	42.0	1.8×10^{13}	2.5×10^{01}
42 ↔ 43 + H_2O	50.8	4.9×10^{13}	2.2×10^{-01}	40.1	2.4×10^{08}	1.1×10^{-03}
3 ↔ 44	33.0	6.4×10^{10}	3.0×10^{01}	39.1	2.5×10^{12}	2.2×10^{01}
44 ↔ 45 + H_2O	66.7	1.0×10^{14}	1.4×10^{-05}	11.3	6.3×10^{07}	4.0×10^{04}
45 ↔ 43	25.0	1.3×10^{11}	1.1×10^{04}	71.2	5.0×10^{12}	3.5×10^{-08}

[a] E_A in kcal/mol; for unimolecular reactions, the units of A and k are s^{-1}; for bimolecular reactions, the units of A and k are M^{-1} s^{-1}

proposed to occur in glucose or cellulose pyrolysis and are less likely than the forms involving the more electrophilic C1. Thus, 2,6- and 3,6-anhydrosugars are not included in this study.

Seshadri and Westmoreland investigated the formation of pyranose levoglucosan via loss of the C1 or C6 hydroxyl group, with a lower barrier when the C1 hydroxyl is lost.[28] While the path to **40** from **1** is clear, it remained less clear if and how **40** can be formed from α-D-glucose (**2**). We found a one-step mechanism for α-D-glucose dehydration to **40** via loss of the C6 hydroxyl group but with an E_A value of 84.3 kcal/mol compared to 48.2 kcal/mol for β-D-glucose to **40** via loss of the anomeric hydroxyl group. The orientation of the anomeric hydroxyl group prevents one-step dehydration of α-D-glucose to **40** by loss of the anomeric hydroxyl group. However, we found that there is a two-step mechanism for α-D-glucose to form **40** with a loss of the anomeric hydroxyl group (Figure 4A). In the first step, the anomeric hydroxyl group abstracts the anomeric hydrogen, resulting in a carbene (**41**). The presence of a lone pair on C1 was verified with NBO. The second step involves nucleophilic attack of O6 on C1, in which the O6 hydrogen is transferred to C1. This two-step path has an E_A value of 76.5 kcal/mol for the first step and 24.9 kcal/mol for the second step. Thus, while the barrier for the two-step mechanism of **2** to **40** is lower than for the one-step **2** to **40** mechanism, E_A is 28 kcal/mol higher than for the **1** to **40** one-step mechanism (relative free energies are shown in Figure 4A and kinetic parameters in Table 4), suggesting that levoglucosan would be predominantly formed from the β-D-glucose anomer.

Seshadri and Westmoreland also investigated the formation of the furanose form of levoglucosan (**43**) from β-D-glucofuranose (**42**) (Figure 4B). We investigated whether **43** could also be formed from α-D-glucofuranose (**44**). As with the formation of **40**, the lowest-energy path we obtained for **44** to **43** also proceeded by a carbene intermediate (**45**). Figure 4B includes the formation of the furanose forms of glucose from open D-glucose, and Table 4 displays the kinetic parameters.

Pyrolysis Results. The above QM studies reveal that some reaction paths from α- or β-D-glucose have similar elementary steps and reaction barriers, such as ring opening, while others are dissimilar, notably the formation of pyranose levoglucosan (**40**; Figure 4). To determine whether differences in mechanism impact observed yields, glucose samples were pyrolyzed containing different anomeric ratios of glucopyranose, specifically either 96% α-D-glucose or 85% β-D-glucose.

As mentioned in the Experimental Methods section, the particle size was held to a specific size, 300−500 μm. The sample mass was also maintained in the range of ∼300−450 μg. The major pyrolysis products are shown in Figure 5 with the full product slate provided in Table S8 of the Supporting Information.

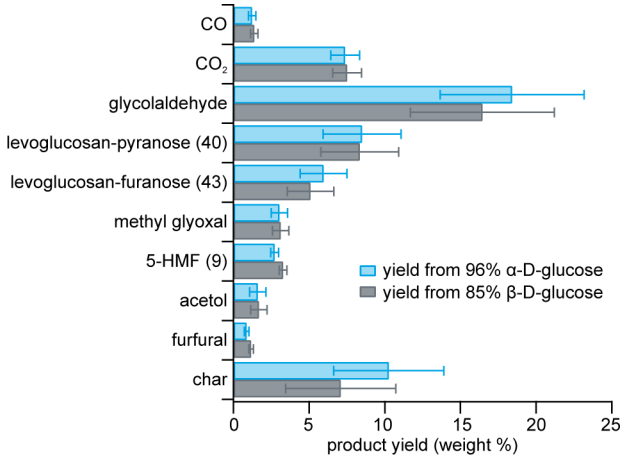

Figure 5. Key pyrolysis product yields of samples rich in either α-D-glucose (light blue) or β-D-glucose (gray). A full list of product yields is included in Table S8 of the Supporting Information.

As evidenced by the major product yields, there is no significant difference between α- or β-D-glucose pyrolysis. Levoglucosan yield was 8.50 ± 0.35 wt % from α-D-glucose and 8.34 ± 2.57 wt % from β-D-glucose, while HMF yield was 2.72 ± 0.29 wt % and 3.28 ± 0.26 wt % from α- and β-D-glucose, respectively. Another major product, glycolaldehyde, was 18.42 ± 0.22 wt % from α-D-glucose and 16.45 ± 4.76 wt % from β-D-glucose. Among the solid and gaseous products from α-D-glucose, char was 10.26 ± 3.90, CO was 1.24 ± 0.16, and CO_2 was 7.38 ± 1.83 wt %. The yields were 7.09 ± 3.64, 1.37 ± 0.24, and 7.51 ± 0.95 wt %, respectively, from β-D-glucose. The yields presented in this study for pyrolysis of either glucose anomer are comparable with previous studies wherein anomer considerations were not explicitly taken into account.[7]

DISCUSSION AND CONCLUSIONS

This work represents the most comprehensive study to date of elementary mechanisms for glucose conversion to 5-HMF under pyrolysis conditions, in addition to a comprehensive study of unimolecular glucose 1,2-dehydration reactions and conversion to the pyranose and furanose forms of levoglucosan. Because the frequency factors for a given reaction type are relatively similar, some conclusions about the dominant pathways can be made based on relative energy barriers

alone. At 500 °C, an energy barrier difference of 3.5 kcal/mol corresponds to an order of magnitude difference in rate coefficient, which provides a metric for evaluating the significance of energy barrier differences. For example, the carbaldehyde bypass step reported here has a rate coefficient 7 orders of magnitude greater than the competing step in the "via fructose" path from glucose to 5-HMF, making it more kinetically significant. We also identified a more direct path from glucose to 5-HMF that avoids an acyclic intermediate. This offers an attractive target for future experimental and computational catalyst design studies,[4,78−81] as it offers a potentially more selective route to producing more of this valuable species.

An interesting finding from the investigation of competing glucose to 5-HMF reaction routes comes from comparing kinetic parameters for reactions of epimers for species other than α- and β-D-glucose. Epimers of **5**, **7**, and **14** have very similar free energies for their local minima but can greatly diverge in energy barrier heights, as demonstrated by the more than 30 kcal/mol difference in E_A values between dehydration to **8** from *trans*-**7** or *cis*-**7**. These differences serve as a reminder of the importance of investigating all relevant stereoisomers when determining rate parameters for elementary steps.

The comparison of different 1,2-dehydration reactions emphasizes the importance of adjacent functional groups in determining reaction kinetics. Dehydration of **1** to **23** clearly illustrates this phenomenon. In this reaction, delocalization of the β-D-glucose O5 lone pairs stabilizes hydroxyl group loss from the adjacent C1. As a result, the rate coefficient is 4 orders of magnitude greater than other β-D-glucose 1,2-dehydration reactions. These considerations are key when extrapolating kinetics calculated on small model molecules[38] to larger molecules with adjacent electron-donating or accepting groups. The comparison of routes to pyranose levoglucosan from α- and β-D-glucose and furanose levoglucosan from α- and β-D-glucofuranose emphasizes the importance of stereochemistry in reaction kinetics.

The differences in mechanisms to form pyranose levoglucosan from α- and β-D-glucose also provide a means of testing whether it is only necessary to consider β-D-glucose in investigating pyrolysis of its polymer. Because pyranose levoglucosan is more readily formed from β-D-glucose than α-D-glucose, we would expect one of two results from pyrolyzing glucose rich in each anomer: either more pyranose levoglucosan would be formed from a sample richer in β-D-glucose than from a sample richer in α-D-glucose or the differences would be statistically insignificant. The latter result was obtained, implying that at pyrolysis conditions, the anomers are in quasi-equilibrium. This result is consistent with studies at lower temperatures (151 and 165 °C) that demonstrated anhydrous mutarotation.[82] A comparison of the energy barriers for anomeric interconversion versus levoglucosan formation reveals that anomer interconversion should be expected; the E_A values for the ring opening and closing required for anomer interconversion are approximately 47 and 35 kcal/mol, respectively, while E_A for β-D-glucose dehydration to pyranose levoglucosan is slightly higher at 48 kcal/mol. Thus, the system is expected to have sufficient energy at pyrolysis conditions for all of these reactions to occur. In fact, early studies found trace evidence of both α- and β-D-glucose in cellulose pyrolysis.[18] These data reinforce our finding that participation of α-D-glucose in the glucose pyrolysis reaction network cannot be summarily dismissed as irrelevant. Overall, this work increases our mechanistic insight into important glucose and thus cellulose pyrolysis reactions and the effect of stereochemistry on its kinetics.

■ ASSOCIATED CONTENT

Supporting Information

Complete ref 43; low-energy "boomerang TS" for isomerization of prop-1-ene 1,2,3-triol to glyceraldehyde; images along the reaction path for **1** to **17** and **2** to **7**; 3D images, atomic coordinates, electronic energy, enthalpy, and free energy (absolute and relative) for all structures; and experimental products observed along with GC retention times, mass spectrometry major fragments, and calibration ranges. This material is available free of charge via the Internet at http://pubs.acs.org.

■ AUTHOR INFORMATION

Corresponding Authors

*E-mail: bshanks@iastate.edu (B.H.S.).
*E-mail: broadbelt@northwestern.edu (L.J.B.).

Notes

The authors declare no competing financial interest.

■ ACKNOWLEDGMENTS

This work was supported by the National Advanced Biofuels Consortium (NABC), which is funded by the Department of Energy (DOE), Office of Energy Efficiency and Renewable Energy (EERE) through the Office of Biomass Program, Grant DE-EE0003044. This research used computational resources of the National Energy Research Scientific Computing Center, which is supported by the Office of Science of the U.S. DOE under Contract DE-AC02-05CH11231 and NREL Computational Sciences Center supported by the DOE Office of EERE under Contract DE-AC36-08GO28308. H.M. thanks Chris Mayes for helpful scripts. H.M. was supported by the DOE Computational Science Graduate Fellowship (CSGF), which is provided under Grant DE-FG02-97ER25308, and the ARCS Foundation Inc., Chicago Chapter.

■ REFERENCES

(1) Ragauskas, A. J.; Williams, C. K.; Davison, B. H.; Britovsek, G.; Cairney, J.; Eckert, C. A.; Frederick, W. J., Jr.; Hallett, J. P.; Leak, D. J.; Liotta, C. L.; Mielenz, J. R.; Murphy, R.; Templer, R.; Tschaplinski, T. The path forward for biofuels and biomaterials. *Science* **2006**, *311*, 484−489.

(2) Bridgwater, A. V.; Peacocke, G. V. C. Fast pyrolysis processes for biomass. *Renew. Sust. Energy Rev.* **2000**, *4*, 1−73.

(3) Czernik, S.; Bridgwater, A. Overview of applications of biomass fast pyrolysis oil. *Energy Fuels* **2004**, *18*, 590−598.

(4) Mohan, D.; Pittman, C. U.; Steele, P. H. Pyrolysis of wood/biomass for bio-oil: A critical review. *Energy Fuels* **2006**, *20*, 848−889.

(5) Regalbuto, J. R. Cellulosic biofuels—Got gasoline? *Science* **2009**, *325*, 822−824.

(6) Kersten, S.; Garcia-Perez, M. Recent developments in fast pyrolysis of ligno-cellulosic materials. *Curr. Opin. Biotechnol.* **2013**, *24*, 414−420.

(7) Patwardhan, P. R.; Satrio, J. A.; Brown, R. C.; Shanks, B. H. Product distribution from fast pyrolysis of glucose-based carbohydrates. *J. Anal. Appl. Pyrolysis* **2009**, *86*, 323−330.

(8) Shen, D. K.; Gu, S. The mechanism for thermal decomposition of cellulose and its main products. *Bioresour. Technol.* **2009**, *100*, 6496−6504.

(9) Wang, S.; Guo, X.; Liang, T.; Zhou, Y.; Luo, Z. Mechanism research on cellulose pyrolysis by Py-GC/MS and subsequent density functional theory studies. *Bioresour. Technol.* **2012**, *104*, 722−728.
(10) Paulsen, A. D.; Mettler, M. S.; Dauenhauer, P. J. The role of sample dimension and temperature in cellulose pyrolysis. *Energy Fuels* **2013**, *27*, 2126−2134.
(11) Lin, Y.-C.; Cho, J.; Tompsett, G. A.; Westmoreland, P. R.; Huber, G. W. Kinetics and mechanism of cellulose pyrolysis. *J. Phys. Chem. C* **2009**, *113*, 20097−20107.
(12) Vinu, R.; Broadbelt, L. J. A mechanistic model of fast pyrolysis of glucose-based carbohydrates to predict bio-oil composition. *Energy Environ. Sci.* **2012**, *5*, 9808−9826.
(13) Mettler, M. S.; Vlachos, D. G.; Dauenhauer, P. J. Top ten fundamental challenges of biomass pyrolysis for biofuels. *Energy Environ. Sci.* **2012**, *5*, 7797−7809.
(14) Broadbelt, L. J.; Pfaendtner, J. Lexicography of kinetic modeling of complex reaction networks. *AIChE J.* **2005**, *51*, 2112−2121.
(15) Lin, T.; Goos, E.; Riedel, U. A sectional approach for biomass: Modelling the pyrolysis of cellulose. *Fuel Process. Technol.* **2013**, *115*, 246−253.
(16) Shafizadeh, F. Introduction to pyrolysis of biomass. *J. Anal. Appl. Pyrolysis* **1982**, *3*, 283−305.
(17) Mayes, H. B.; Broadbelt, L. J. Unraveling the reactions that unravel cellulose. *J. Phys. Chem. A* **2012**, *116*, 7098−7106.
(18) Shafizadeh, F.; Fu, Y. L. Pyrolysis of cellulose. *Carbohydr. Res.* **1973**, *29*, 113−122.
(19) Boon, J. J.; Pastorova, I.; Botto, R. E.; Arisz, P. W. Structural studies on cellulose pyrolysis and cellulose chars by PYMS, PYGCMS, FTIR, NMR and by wet chemical techniques. *Biomass Bioenergy* **1994**, *7*, 25−32.
(20) Sanders, E. B.; Goldsmith, A. I.; Seeman, J. I. A model that distinguishes the pyrolysis of D-glucose, D-fructose, and sucrose from that of cellulose. Application to the understanding of cigarette smoke formation. *J. Am. Chem. Soc.* **2003**, *66*, 29−50.
(21) Paine, J. B., III; Pithawalla, Y. B.; Naworal, J. D. Carbohydrate pyrolysis mechanisms from isotopic labeling. Part 2. The pyrolysis of D-glucose: General disconnective analysis and the formation of C1 and C2 carbonyl compounds by electrocyclic fragmentation mechanisms. *J. Anal. Appl. Pyrolysis* **2008**, *82*, 10−41.
(22) Paine, J. B., III; Pithawalla, Y. B.; Naworal, J. D. Carbohydrate pyrolysis mechanisms from isotopic labeling. Part 3. The pyrolysis of D-glucose: Formation of C3 and C4 carbonyl compounds and a cyclopentenedione isomer by electrocyclic fragmentation mechanisms. *J. Anal. Appl. Pyrolysis* **2008**, *82*, 42−69.
(23) Paine, J. B., III; Pithawalla, Y. B.; Naworal, J. D. Carbohydrate pyrolysis mechanisms from isotopic labeling. Part 4. The pyrolysis of D-glucose: The formation of furans. *J. Anal. Appl. Pyrolysis* **2008**, *83*, 37−63.
(24) Huang, J.; Liu, C.; Wei, S.; Huang, X.; Li, H. Density functional theory studies on pyrolysis mechanism of β-D-glucopyranose. *J. Mol. Struct.: THEOCHEM* **2010**, *958*, 64−70.
(25) Shen, C.; Zhang, I. Y.; Fu, G.; Xu, X. Pyrolysis of D-glucose to acrolein. *Chin. J. Chem. Phys.* **2011**, *24*, 249−252.
(26) Jadhav, H.; Pedersen, C. M.; Sølling, T.; Bols, M. 3-Deoxyglucosone is an intermediate in the formation of furfurals from D-glucose. *ChemSusChem* **2011**, *4*, 1049−1051.
(27) Assary, R. S.; Curtiss, L. A. Comparison of sugar molecule decomposition through glucose and fructose: A high-level quantum chemical study. *Energy Fuels* **2012**, *26*, 1344−1352.
(28) Seshadri, V.; Westmoreland, P. R. Concerted reactions and mechanism of glucose pyrolysis and implications for cellulose kinetics. *J. Phys. Chem. A* **2012**, *116*, 11997−12013.
(29) Lu, Q.; Liao, H.-t.; Zhang, Y.; Zhang, J.-j.; Dong, C.-q. Reaction mechanism of low-temperature fast pyrolysis of fructose to produce 5-hydroxymethyl furfural. *J. Fuel Chem. Technol.* **2013**, *41*, 1070−1076.
(30) Zhang, Y.; Liu, C.; Xie, H. Mechanism studies on β-D-glucopyranose pyrolysis by density functional theory methods. *J. Anal. Appl. Pyrolysis* **2014**, *105*, 23−34.
(31) Ponder, G. R.; Richards, G. N. Pyrolysis of inulin, glucose, and fructose. *Carbohydr. Res.* **1993**, *244*, 341−359.
(32) Kamm, B. Production of platform chemicals and synthesis gas from biomass. *Angew. Chem., Int. Ed.* **2007**, *46*, 5056−5058.
(33) Alonso, D. M.; Bond, J. Q.; Dumesic, J. A. Catalytic conversion of biomass to biofuels. *Green Chem.* **2010**, *12*, 1493−1513.
(34) Bozell, J. J.; Petersen, G. R. Technology development for the production of biobased products from biorefinery carbohydrates−the US Department of Energy's "top 10" revisited. *Green Chem.* **2010**, *12*, 539−554.
(35) Rosatella, A. A.; Simeonov, S. P.; Frade, R. F. M.; Afonso, C. A. M. 5-Hydroxymethylfurfural (HMF) as a building block platform: Biological properties, synthesis and synthetic applications. *Green Chem.* **2011**, *13*, 754−793.
(36) Gallezot, P. Conversion of biomass to selected chemical products. *Chem. Soc. Rev.* **2012**, *41*, 1538−1558.
(37) Saha, B.; Abu-Omar, M. M. Advances in 5-hydroxymethylfurfural production from biomass in biphasic solvents. *Green Chem.* **2014**, *16*, 24−38.
(38) Nimlos, M. R.; Blanksby, S. J.; Ellison, G. B.; Evans, R. J. Enhancement of 1,2-dehydration of alcohols by alkali cations and protons: A model for dehydration of carbohydrates. *J. Anal. Appl. Pyrolysis* **2003**, *66*, 3−27.
(39) Zugenmaier, P. *Crystalline Cellulose and Derivatives: Characterization and Structures*; Springer-Verlag: Berlin, 2008.
(40) Angyal, S. J. The composition and conformation of sugars in solution. *Angew. Chem., Int. Ed.* **1969**, *8*, 157−166.
(41) Zhu, Y.; Zajicek, J.; Serianni, A. S. Acyclic forms of [1-^{13}C] aldohexoses in aqueous solution: Quantitation by ^{13}C NMR and deuterium isotope effects on tautomeric equilibria. *J. Org. Chem.* **2001**, *66*, 6244−6251.
(42) Qian, X. Mechanisms and energetics for acid catalyzed β-D-glucose conversion to 5-hydroxymethylfurfurl. *J. Phys. Chem. A* **2011**, *115*, 11740−11748.
(43) Frisch, M. J. et al. Gaussian 09 Revision C.01. Gaussian, Inc.: Wallingford, CT, 2010.
(44) Zhao, Y.; Truhlar, D. G. The M06 suite of density functionals for main group thermochemistry, thermochemical kinetics, noncovalent interactions, excited states, and transition elements: Two new functionals and systematic testing of four M06-class functionals and 12 other functionals. *Theor. Chem. Acc.* **2008**, *120*, 215−241.
(45) Zhao, Y.; Truhlar, D. G. Exploring the limit of accuracy of the global hybrid meta density functional for main-group thermochemistry, kinetics, and noncovalent interactions. *J. Chem. Theory Comput.* **2008**, *4*, 1849−1868.
(46) Sameera, W. M. C.; Pantazis, D. A. A hierarchy of methods for the energetically accurate modeling of isomerism in monosaccharides. *J. Chem. Theory Comput.* **2012**, *8*, 2630−2645.
(47) Krishnan, R.; Binkley, J. S.; Seeger, R.; Pople, J. A. Self-consistent molecular orbital methods. XX. A basis set for correlated wave functions. *J. Chem. Phys.* **1980**, *72*, 650−654.
(48) Frisch, M. J.; Pople, J. A.; Binkley, J. S. Self-consistent molecular orbital methods 25. Supplementary functions for Gaussian basis sets. *J. Chem. Phys.* **1984**, *80*, 3265−3269.
(49) Glendening, E. D.; Landis, C. R.; Weinhold, F. Natural bond orbital methods. *WIREs Comput. Mol. Sci.* **2012**, *2*, 1−42.
(50) Glendening, E.; Badenhoop, J. K.; Reed, A. E.; Carpenter, J. E.; Bohmann, J. A.; Morales, C. M.; Landis, C. R.; Weinhold, F. *NBO 6.0.*; Theoretical Chemistry Institute: Madison, WI, 2013.
(51) Hratchian, H. P.; Schlegel, H. B. Accurate reaction paths using a Hessian based predictor-corrector integrator. *J. Chem. Phys.* **2004**, *120*, 9918−9924.
(52) Hratchian, H. P.; Schlegel, H. B. In *Theory and Applications of Computational Chemistry: The First Forty Years*; Dykstra, C. E., Frenking, G., Kim, K. S., Scuseria, G., Eds.; Elsevier Science: Amsterdam, 2005; pp 195−249.
(53) Hratchian, H. P.; Schlegel, H. B. Using Hessian updating to increase the efficiency of a Hessian based predictor-corrector reaction path following method. *J. Chem. Theory Comput.* **2005**, *1*, 61−69.

(54) Collins, M. A. Molecular potential-energy surfaces for chemical reaction dynamics. *Theor. Chem. Acc.* **2002**, *108*, 313−324.
(55) Merrick, J. P.; Moran, D.; Radom, L. An evaluation of harmonic vibrational frequency scale factors. *J. Phys. Chem. A* **2007**, *111*, 11683−11700.
(56) Moore, J. W.; Pearson, R. G. *Kinetics and Mechanism*, 3rd ed.; John Wiley & Sons: New York, 1981.
(57) Piskorz, J.; Majerski, P.; Radlein, D.; Vladars-Usas, A.; Scott, D. S. Flash Pyrolysis of cellulose for production of anhydro-oligomers. *J. Anal. Appl. Pyrolysis* **2000**, *56*, 145−166.
(58) Tomasi, J.; Mennucci, B.; Cammi, R. Quantum mechanical continuum solvation models. *Chem. Rev.* **2005**, *105*, 2999−3093.
(59) Cattoir, F. R.; Parks, G. S. Studies on glass III. The dielectric constants of glassy and liquid glucose. *J. Phys. Chem.* **1929**, *33*, 879−882.
(60) Chan, R. K.; Pathmanathan, K.; Johari, G. P. Dielectric relaxations in the liquid and glassy states of glucose and its water mixtures. *J. Phys. Chem.* **1986**, *90*, 6358−6362.
(61) Calkins, C. R. Studies of dielectric properties of chemical pulps: III. Dielectric properties of cellulose. *TAPPI* **1950**, *33*, 278−285.
(62) Reyes-de Corcuera, J. I.; Teruel, M. A.; Jenkins, D. M. Crystallization of β-D-glucose and analysis with a simple glucose biosensor. *J. Chem. Educ.* **2009**, *86*, 9−11.
(63) Hudson, C. S.; Dale, J. K. Studies on the forms of D-glucose and their mutarotation. *J. Am. Chem. Soc.* **1917**, *39*, 320−328.
(64) Perez Locas, C.; Yaylayan, V. A. Isotope labeling studies on the formation of 5-(hydroxymethyl)-2-furaldehyde (HMF) from sucrose by pyrolysis-GC/MS. *J. Agric. Food Chem.* **2008**, *56*, 6717−6723.
(65) Karinen, R.; Vilonen, K.; Niemelä, M. Biorefining: Heterogeneously catalyzed reactions of carbohydrates for the production of furfural and hydroxymethylfurfural. *ChemSusChem* **2011**, *4*, 1002−1016.
(66) Assary, R. S.; Redfern, P. C.; Greeley, J.; Curtiss, L. A. Mechanistic insights into the decomposition of fructose to hydroxy methyl furfural in neutral and acidic environments using high-level quantum chemical methods. *J. Phys. Chem. B* **2011**, *115*, 4341−4349.
(67) McNaught, A. D. Nomenclature of carbohydrates (IUPAC Recommendations 1996). *Pure Appl. Chem.* **1996**, *68*, 1919−2008.
(68) Mayes, H. B.; Tian, J.; Nolte, M. W.; Shanks, B. H.; Beckham, G. T.; Gnanakaran, S.; Broadbelt, L. J. Sodium ion interactions with aqueous glucose: Insights from quantum mechanics, molecular dynamics, and experiment. *J. Phys. Chem. B* **2014**, *118*, 1990−2000.
(69) Rasrendra, C. B.; Makertihartha, I. G. B. N.; Adisasmito, S.; Heeres, H. J. Green chemicals from D-glucose: Systematic studies on catalytic effects of inorganic salts on the chemo-selectivity and yield in aqueous solutions. *Top. Catal.* **2010**, *53*, 1241−1247.
(70) Pagán-Torres, Y. J.; Wang, T.; Gallo, J. M. R.; Shanks, B. H.; Dumesic, J. A. Production of 5-hydroxymethylfurfural from glucose using a combination of Lewis and Brønsted acid catalysts in water in a biphasic reactor with an alkylphenol solvent. *ACS Catal.* **2012**, *2*, 930−934.
(71) Kobayashi, H.; Fukuoka, A. Synthesis and utilisation of sugar compounds derived from lignocellulosic biomass. *Green Chem.* **2013**, *15*, 1740−1763.
(72) Combs, E.; Cinlar, B.; Pagan-Torres, Y.; Dumesic, J. A.; Shanks, B. H. Influence of alkali and alkaline earth metal salts on glucose conversion to 5-hydroxymethylfurfural in an aqueous system. *Catal. Commun.* **2013**, *30*, 1−4.
(73) Patwardhan, P. R.; Dalluge, D. L.; Shanks, B. H.; Brown, R. C. Distinguishing primary and secondary reactions of cellulose pyrolysis. *Bioresour. Technol.* **2011**, *102*, 5265−5269.
(74) Schneider, B.; Lichtenthaler, F. W.; Steinle, G.; Schiweck, H. Studies on ketoses, 1 distribution of furanoid and pyranoid tautomers of D-fructose in water, dimethyl sulfoxide, and pyridine via ^{1}H NMR intensities of anomeric hydroxy groups in [D_6]DMSO. *Liebigs Ann. Chem.* **1985**, *1985*, 2443Ð−2453.
(75) Kilzer, F. J.; Broido, A. Speculation on the nature of cellulose pyrolysis. *Pyrodynamics* **1965**, *2*, 151−163.
(76) Mayes, H. B.; Broadbelt, L. J.; Beckham, G. T. How sugars pucker: Electronic structure calculations map the kinetic landscape of five biologically paramount monosaccharides and their implications for enzymatic catalysis. *J. Am. Chem. Soc.* **2014**, *136*, 1008−1022.
(77) Zhang, M.; Geng, Z.; Yu, Y. Density functional theory (DFT) study on the dehydration of cellulose. *Energy Fuels* **2011**, *25*, 2664−2670.
(78) Carlson, T. R.; Vispute, T. P.; Huber, G. W. Green gasoline by catalytic fast pyrolysis of solid biomass derived compounds. *ChemSusChem* **2008**, *1*, 397−400.
(79) Nørskov, J. K.; Bligaard, T.; Rossmeisl, J.; Christensen, C. H. Towards the computational design of solid catalysts. *Nat. Chem.* **2009**, *1*, 37−46.
(80) French, R.; Czernik, S. Catalytic pyrolysis of biomass for biofuels production. *Fuel Process. Technol.* **2010**, *91*, 25−32.
(81) Baldwin, R. M.; Magrini-Bair, K. A.; Nimlos, M. R.; Pepiot, P.; Donohoe, B. S.; Hensley, J. E.; Phillips, S. D. Current research on thermochemical conversion of biomass at the National Renewable Energy Laboratory. *Appl. Catal., B* **2012**, *115*−*116*, 320−329.
(82) Broido, A.; Houminer, Y.; Patai, S. Pyrolytic reactions of carbohydrates. Part I. Mutarotation of molten D-glucose. *J. Chem. Soc. B* **1966**, *0*, 411−414.